

**Special Issue: Manufacturing of Advanced
Biodegradable Polymeric Components**

Guest Editors: Prof. Roberto Pantani (University of Salerno) and
Prof. Lih-Sheng Turng (University of Wisconsin-Madison)

EDITORIAL

Manufacturing of advanced biodegradable polymeric components

R. Pantani and L.-S. Turng, *J. Appl. Polym. Sci.* 2015, DOI: [10.1002/app.42889](https://doi.org/10.1002/app.42889)

REVIEWS

Heat resistance of new biobased polymeric materials, focusing on starch, cellulose, PLA, and PHA

N. Peelman, P. Ragaert, K. Ragaert, B. De Meulenaer, F. Devlieghere and Ludwig Cardon, *J. Appl. Polym. Sci.* 2015, DOI: [10.1002/app.42305](https://doi.org/10.1002/app.42305)

Recent advances and migration issues in biodegradable polymers from renewable sources for food packaging

P. Scarfato, L. Di Maio and L. Incarnato, *J. Appl. Polym. Sci.* 2015, DOI: [10.1002/app.42597](https://doi.org/10.1002/app.42597)

3D bioprinting of photocrosslinkable hydrogel constructs

R. F. Pereira and P. J. Bartolo, *J. Appl. Polym. Sci.* 2015, DOI: [10.1002/app.42458](https://doi.org/10.1002/app.42458)

ARTICLES

Largely toughening biodegradable poly(lactic acid)/thermoplastic polyurethane blends by adding MDI

F. Zhao, H.-X. Huang and S.-D. Zhang, *J. Appl. Polym. Sci.* 2015, DOI: [10.1002/app.42511](https://doi.org/10.1002/app.42511)

Solubility factors as screening tools of biodegradable toughening agents of polylactide

A. Ruellan, A. Guinault, C. Sollogoub, V. Ducruet and S. Domenek, *J. Appl. Polym. Sci.* 2015, DOI: [10.1002/app.42476](https://doi.org/10.1002/app.42476)

Current progress in the production of PLA-ZnO nanocomposites: Beneficial effects of chain extender addition on key properties

M. Murariu, Y. Paint, O. Murariu, J.-M. Raquez, L. Bonnaud and P. Dubois, *J. Appl. Polym. Sci.* 2015, DOI: [10.1002/app.42480](https://doi.org/10.1002/app.42480)

Oriented polyvinyl alcohol films using short cellulose nanofibrils as a reinforcement

J. Peng, T. Ellingham, R. Sabo, C. M. Clemons and L.-S. Turng, *J. Appl. Polym. Sci.* 2015, DOI: [10.1002/app.42283](https://doi.org/10.1002/app.42283)

Biorenewable polymer composites from tall oil-based polyamide and lignin-cellulose fiber

K. Liu, S. A. Madbouly, J. A. Schrader, M. R. Kessler, D. Grewell and W. R. Graves, *J. Appl. Polym. Sci.* 2015, DOI: [10.1002/app.42592](https://doi.org/10.1002/app.42592)

Dual effect of chemical modification and polymer precoating of flax fibers on the properties of the short flax fiber/poly(lactic acid) composites

M. Kodal, Z. D. Topuk and G. Ozkoc, *J. Appl. Polym. Sci.* 2015, DOI: [10.1002/app.42564](https://doi.org/10.1002/app.42564)

Effect of processing techniques on the 3D microstructure of poly(L-lactic acid) scaffolds reinforced with wool keratin from different sources

D. Puglia, R. Ceccolini, E. Fortunati, I. Armentano, F. Morena, S. Martino, A. Aluigi, L. Torre and J. M. Kenny, *J. Appl. Polym. Sci.* 2015, DOI: [10.1002/app.42890](https://doi.org/10.1002/app.42890)

Batch foaming poly(vinyl alcohol)/microfibrillated cellulose composites with CO₂ and water as co-blowing agents

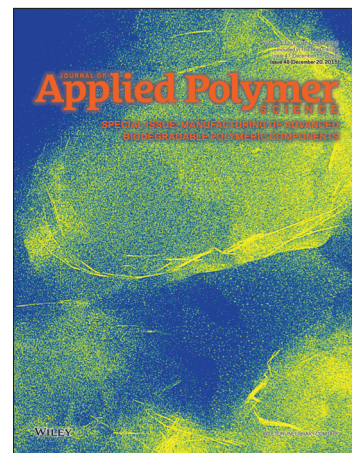
N. Zhao, C. Zhu, L. H. Mark, C. B. Park and Q. Li, *J. Appl. Polym. Sci.* 2015, DOI: [10.1002/app.42551](https://doi.org/10.1002/app.42551)

Foaming behavior of biobased blends based on thermoplastic gelatin and poly(butylene succinate)

M. Oliviero, L. Sorrentino, L. Caferio, B. Galzerano, A. Sorrentino and S. Iannace, *J. Appl. Polym. Sci.* 2015, DOI: [10.1002/app.42704](https://doi.org/10.1002/app.42704)

Reactive extrusion effects on rheological and mechanical properties of poly(lactic acid)/poly[(butylene succinate)-co-adipate]/epoxy chain extender blends and clay nanocomposites

A. Mirzadeh, H. Ghasemi, F. Mahrous and M. R. Kamal, *J. Appl. Polym. Sci.* 2015, DOI: [10.1002/app.42664](https://doi.org/10.1002/app.42664)



**Special Issue: Manufacturing of Advanced
Biodegradable Polymeric Components**

Guest Editors: Prof. Roberto Pantani (University of Salerno) and
Prof. Lih-Sheng Turng (University of Wisconsin-Madison)

Rotational molding of biodegradable composites obtained with PLA reinforced by the wooden backbone of opuntia ficus indica cladodes

A. Greco and A. Maffezzoli, *J. Appl. Polym. Sci.* 2015, DOI: [10.1002/app.42447](https://doi.org/10.1002/app.42447)

Foam injection molding of poly(lactic) acid: Effect of back pressure on morphology and mechanical properties

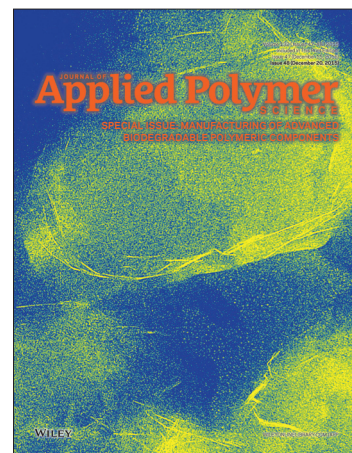
V. Volpe and R. Pantani, *J. Appl. Polym. Sci.* 2015, DOI: [10.1002/app.42612](https://doi.org/10.1002/app.42612)

Modification and extrusion coating of polylactic acid films

H.-Y. Cheng, Y.-J. Yang, S.-C. Li, J.-Y. Hong and G.-W. Jang, *J. Appl. Polym. Sci.* 2015, DOI: [10.1002/app.42472](https://doi.org/10.1002/app.42472)

Processing and properties of biodegradable compounds based on aliphatic polyesters

M. R. Nobile, P. Cerruti, M. Malinconico and R. Pantani, *J. Appl. Polym. Sci.* 2015, DOI: [10.1002/app.42481](https://doi.org/10.1002/app.42481)



Dual effect of chemical modification and polymer precoating of flax fibers on the properties of short flax fiber/poly(lactic acid) composites

Mehmet Kodal, Zeynep Demir Topuk, Guralp Ozkoc

Department of Chemical Engineering, Kocaeli University, Izmit/Kocaeli 41380, Turkey

Correspondence to: G. Ozkoc (E-mail: guralp.ozkoc@kocaeli.edu.tr)

ABSTRACT: Polymer precoated and chemically modified short flax fiber (SFF)/poly(lactic acid) (PLA) composites were successfully produced. The main focus of this study was to investigate the effects of the combinatorial use of chemical modification methods of flax fiber, such as alkaline treatment and silane coupling agents, together with polymer precoating as the film former on the physical and mechanical properties for PLA/SFF composites. The chemically modified flax fibers were characterized by X-ray diffraction (XRD), X-ray photoelectron spectroscopy (XPS), and scanning electron microscopy. It was revealed from XRD analysis that alkaline treatment resulted in change in the cellulose I structure to the cellulose II structure because of the removal of the cementing non-cellulosic components. The XPS analysis showed that the silane groups were successfully bonded to the surface of the flax fiber. As the film-former application, PLA was coated on the surface of alkaline or silane-treated flax fiber surfaces via a solution dipping process. The SFF content was kept constant at 25 wt % in the composites that were prepared by means of a 15 mL Xplore Instruments twin-screw compounder. After melt processing, the positive effect of the sizing application on both the alkaline- and silane-treated SFF was observed from the enhanced fiber length distribution. The mechanical properties were examined by means of tensile and impact tests and dynamic mechanical analysis. In addition, the thermal properties obtained from differential scanning calorimetry were discussed as a function of the fiber treatment method. The hydrolysis rate was determined by a weight loss test in a phosphate buffer solution. The results showed that in addition to the positive single influence of the silane coupling agent, the synergetic effect of the film former (i.e., precoated polymer) and silane treatment was observed to improve the performance of the composites. The hydrolysis rate of the polymer-coated flax-based composites was lower than that of uncoated flax fiber composites. In addition, polymer-coated flax fibers could be easily processed like conventional chopped short-glass-fiber composites. © 2015 Wiley Periodicals, Inc. *J. Appl. Polym. Sci.* 2015, 132, 42564.

KEYWORDS: composite; flax fiber; interface; mechanical properties; poly(lactic acid)

Received 16 February 2015; accepted 1 June 2015

DOI: 10.1002/app.42564

INTRODUCTION

With increasing environmental awareness and enforcing legislations, the usage of fully biodegradable polymeric materials has received enormous attention from manufacturers. Conventional polymeric composites are nonbiodegradable and contribute solid waste pollution and a dependency on petroleum-based nonrenewable sources. Ecological composites are produced by the incorporation of a natural renewable fiber to a completely biodegradable biopolymer synthesized from renewable resources, such as cellulosic plastics, aliphatic polyesters, thermoplastic starch, polyhydroxyalkanoates (bacterial polyesters), and soy-based plastics. Natural fiber resources used to obtain reinforcing fiber in bioplastics are sisal, coconut coir, jute, hemp, ramie, palm, cotton, rice husk, bamboo, banana, wood and flax.¹ Among all of the natural fibers, flax is considered to be one of the strongest and easily available fibers that can be replaced

with conventional fibers such as glass fibers.² However, the poor compatibility between highly polar cellulose and the nonpolar matrices are the main disadvantage of flax fibers; this reduces their potential as reinforcing agents in composites, such as automotive applications.^{3,4}

Many renewable and readily biodegradable polymers have excellent properties comparable to many petroleum-based plastics, and in addition, they may be replaced with commodity plastics. However, some of their properties, such as brittleness, low heat distortion temperature, and low melt viscosity, restrict their applications in real life.⁵ Poly(lactic acid) (PLA) is a promising compostable polymer that is synthesized from renewable resources, such as corn, sugar cane, or potatoes. In contrast to conventional plastics that degrade in a hundred years, PLA can biodegrade into carbon dioxide and water in a short period of time.⁶ Above all, PLA is relatively cheap and already

commercially available at different grades from different companies. PLA can be processed in a similar manner to that of polyolefins, especially polypropylene (PP), and other thermoplastics. The properties of PLA can be modified through the use of the cellulosic fibers such as flax. This modification also reduces the cost of the PLA without restricting its biodegradability.^{3,7}

In recent years, flax fiber-reinforced PLA eco-composites have been studied by some researchers.^{8–10} Although these kinds of eco-composites exhibit interesting mechanical properties, the major drawbacks of natural fibers are their poor thermal stability, anisotropic mechanical performances, high moisture absorption, and heterogeneity.^{11,12} In addition, the mechanical performance of these composites is closely related to the quality of the fiber–matrix interface, which defines the amount of stress transferred from the matrix to the fiber. Because PLA is relatively hydrophobic and the flax fiber is hydrophilic, the mechanical properties of composites become insufficient without any surface modification.¹³ To improve the interfacial compatibility, alkali treatment (mercerization), dewaxing, silane modification, acrylation, peroxide treatment, and coatings have been discussed in the literature.^{3,13–16} In the alkaline treatment method, the surface roughness of fibers is increased with NaOH; this results in breakage of the hydrogen bonding in the network structure of the fiber.^{17,18} Lignin, hemicellulose, waxes, and oils that cover the external surface of the fiber cell walls have also been removed by the application of alkaline treatment.^{17,18} In addition, the fiber diameter was reduced, and so, the aspect ratio of the fiber was increased.¹⁹ In addition, alkaline treatment also affects the molecular orientation of cellulose crystallites because of the removal of lignin and hemicellulose.³ In a recent study, Sirvaitiene *et al.*¹⁷ investigated the influence of chemical and/or mechanical treatment on the adhesion interaction of PLA composites reinforced by flax or cotton. It was reported that the tensile strength of PLA biocomposites increased when the flax fiber underwent alkaline treatment. In another study conducted by Aydin *et al.*,³ the effects of alkali treatment on the properties of short flax fiber (SFF)/PLA eco-composites were investigated. They concluded that the modulus of the untreated fiber/PLA composites was higher than that of PLA; on the other hand, the modulus of the alkali-treated flax fiber/PLA composite was lower than that of neat PLA. This reduced modulus of elasticity in the composite was attributed to the weakening of the flax fiber after alkaline treatment.

As mentioned earlier, silane treatment is one of the most applied methods for improving the interfacial adhesion between the fiber and matrix. In this method, silane is hydrolyzed, forms reactive silanols, and is then adsorbed and condensed on the fiber surface (sol–gel process). Thus, the hydrogen bonds formed between the adsorbed silanols and hydroxyl groups of natural fibers improve the mechanical performances of the resulting polymer/fiber composites.¹³ Yuan *et al.*²⁰ used silanized flax fibers as reinforcement in PLA biodegradable composites. They emphasized that with the increases in flax addition from 30 to 50% and silane addition from 1 to 5%, the tensile strength and modulus increased. On the other hand, the flexural strength and modulus first increased and then decreased with increasing flax addition. Le Moigne *et al.*²¹ treated flax fibers

with an epoxide functional organosilane coupling agent, 3-glycidyloxypropyl trimethoxysilane, under various conditions. It was demonstrated that the optimization of the organosilane treatment conditions increased the hydrophobicity of fibers and significantly increased the stiffness, yield, and impact strength of the PLA/flax fiber biocomposites.

In addition to the surface modification by silanes, the utilization of film formers to form a sizing layer is known to be an effective method in the short-glass-fiber industry to protect the fiber from damage during production, handling, and processing.²² It is known that the film former in conjunction with the silane governs the wetting behavior, the resulting interfacial structure, and most of the properties of fiber-based composites materials.^{23,24} In addition, the introduction of polymer coatings (PCs; i.e., film-forming polymer or film former) on the fiber surface can help to separate fibers from each other, eliminate the hydrogen bonding that holds them together, and also induce bond formation between the fibers and the matrix; this results in improved composite properties.^{25,26} Although the influence of the coupling agent on the interfacial mechanical properties of natural fiber composites has been the subject of numerous articles, the effect of the nature of the film former has been very poorly investigated. In a recent study conducted by Altun *et al.*,²⁷ the effects of alkaline treatment and pre-impregnation with a PLA solution on the mechanical and water absorption properties of pine wood flour containing PLA-based green composites were investigated. It was concluded that alkaline treatment and pre-impregnation were effective methods for increasing the mechanical properties, including the tensile modulus and tensile and impact strengths of PLA/wood flour composites.

In this study, by inspiring from the glass fiber technology, we investigated the effects of chemical modification methods applied to flax fiber, such as alkaline treatment and silane coupling agents, in combination with a polymer pre-coating as the film former on the physical and mechanical properties of PLA/SFF composites, for the first time in the literature. The chemically modified flax fibers were characterized by X-ray diffraction (XRD), X-ray photoelectron spectroscopy (XPS), and scanning electron microscopy (SEM). The SFF composites were prepared via twin-screw compounding. The fiber content was kept constant at 25 wt %, but the surface-treatment type was varied. The relationship between the fiber surface treatment and the mechanical properties were focused.

EXPERIMENTAL

Materials

The properties of the materials are given in Table I. The PLA used in the studies was an injection-molding-grade resin with a melt flow index of 18 g/10 min (190°C and 2.16 kg). Flax fibers were obtained from a local producer in Kandira, Turkey. The silane coupling agent and solvents were purchased from Sigma-Aldrich Co. and Albar Chemical Co., respectively.

Treatment of Flax Fibers and Composite Preparation

In alkaline treatment, long flax fibers were first washed with excess ethanol (EtOH) to remove any waxes. A 10% NaOH

Table I. Properties of the Materials Used in the Experiments

Material	Source/trade name	Specifications/properties
PLA	Natureplast (France)/PLI 005	<ul style="list-style-type: none"> Genetically modified organism (GMO)-free PLA for injection molding Melt flow index: 18 g/10 min at 190°C Density: 1.25 g/cm³ Transparent pellets
Flax fiber	Local source (Kandira, Turkey)	<ul style="list-style-type: none"> Tow form Average diameter: 179 ± 95 μm Density: 1.43 g/cm³ Tensile strength: 650 ± 340 MPa Tensile modulus: 43 ± 8.7 GPa
Silane coupling agent	Sigma-Aldrich (Germany)	<ul style="list-style-type: none"> APS
Solvents	Albar Chemical Co. (Kocaeli, Turkey)	<ul style="list-style-type: none"> Ethyl alcohol and chloroform Technical grade

solution was used as the alkaline medium. Before the wet process, the fibers were wrapped around a rectangular frame and dipped into the alkaline solution. After the treatment, the fibers were washed with an excess amount of water. In the following step, the flax fibers were placed in a vacuum oven at 80°C for 3 h to remove the moisture. In the silane treatment, the flax fibers were washed with EtOH and dipped into a 3-aminopropyltrimethoxysilane (APS) solution in a 60% v/v EtOH/water mixture. At the end of 4 h of treatment, the silanized fibers were put in a vacuum oven at 70°C for 48 h for the curing of the silanes. The alkaline- or silane-modified flax fibers were then treated by a 15% PLA solution in chloroform to coat the fiber surface with PLA. Before compounding, the treated flax fibers were chopped to 0.5 cm. The fiber treatment procedure is schematically shown in Figure 1.

The chopped fibers and PLA were melt-compounded in a laboratory-type twin-screw compounder (Xplore Instruments 15 mL microcompounder) at 180°C at 100 rpm to obtain 25 wt % fiber-loaded composites. Before processing, both PLA and the fibers were dried in a vacuum oven at 60°C for 12 h. To prepare standard samples for tensile and impact tests, an Xplore Instruments 12 mL microinjection molding machine was used. The melting temperature (T_m) was 180°C, and the mold temperature

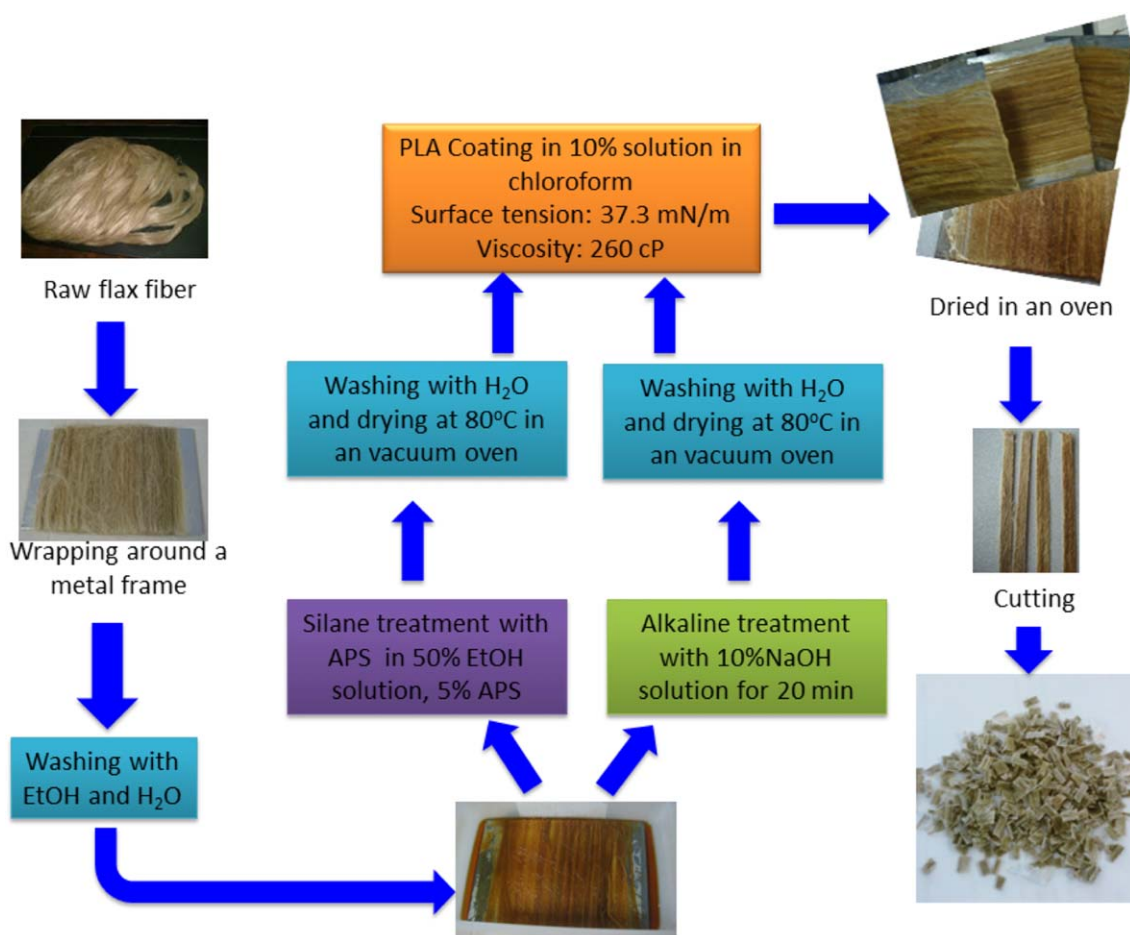


Figure 1. Schematic representation of the flax fiber treatment procedure. [Color figure can be viewed in the online issue, which is available at wileyonlinelibrary.com.]

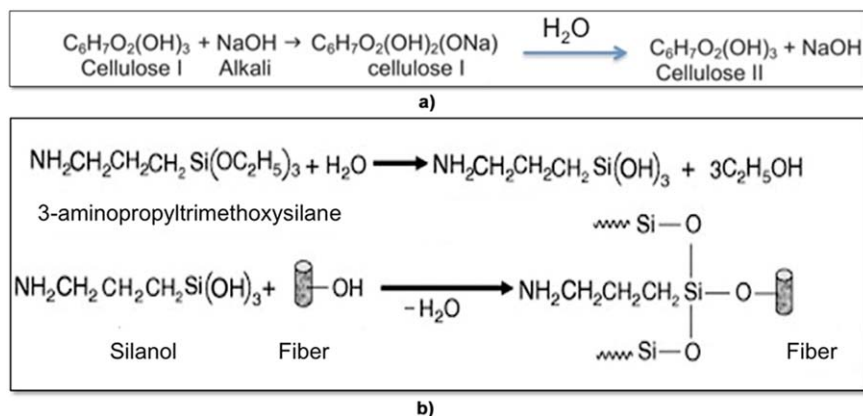


Figure 2. Schematic representation of the (a) alkaline and (b) silane treatments. [Color figure can be viewed in the online issue, which is available at wileyonlinelibrary.com.]

was 25°C. As the control, untreated flax fiber composites were also prepared.

Characterization

To observe the morphological changes in the flax fibers after the treatment procedure, wide-angle XRD analysis was carried out with a Rigaku D/MAX 2200/PC diffractometer with a Cu K α (1.54 Å) radiation source generated at a voltage of 40 kV and a current of 40 mA. The scanning rate was 2°/min. XPS spectra were recorded on a SPECS EA 300 spectrometer with Al K α radiation. The samples were analyzed for the C1s, Si2p, and O1s peaks.

To obtain the fiber length distributions in the resulting composites, injection-molded tensile bars were used. The fibers were separated by the dissolution of the PLA matrix in an excess amount of chloroform and subsequent filtering and drying. The collected fibers were analyzed with an optical microscope (Nikon LV100 POL) at a magnification of 100 \times . At least 400 fibers were measured to obtain the distribution curves.

Tensile tests of the composites were conducted according to ISO 527 5a with a universal tester (Zwick Roell Z005). A 5-kN load cell was used. The crosshead speed of the test was 10 mm/min. Measurements were performed at room temperature with at least five parallel specimens. The Charpy impact tests were conducted with a pendulum type impact tester (Ceast Resil Impactor) with V-notched samples according to ISO 180 at room temperature.

Dynamical mechanical properties were obtained with a Metravib 01dB DMA50 instrument in tensile mode. The frequency of the test was constant at 1 Hz. The temperature was scanned from 25 to 150°C. The temperature ramp in the experiments was 3 K/min.

The flax fiber surfaces after treatments and the interfacial topology after tensile testing in the composites were observed by means of SEM (JEOL JSM-6335F). Before analysis, the sample surfaces were sputter-coated with gold to prevent arching.

Differential scanning calorimetry (DSC; Mettler Toledo DSC1 Star System) was used to monitor the thermal properties of the pure PLA and PLA/flax fiber composites. The samples were

heated from 25 to 180°C at a rate of 10 K/min. The thermal properties were determined from the first heating scan.

Hydrolytic degradation was investigated in a phosphate buffer solution (pH 7.4) through determination of the degradation rate from the weight loss. Samples approximately 0.5 mm in thickness were placed in a bottle containing 25 mL of solution. The solution was refreshed everyday. The bottles were then placed in a water bath that remained at a constant temperature of 60°C during the whole degradation period, and the weights of the samples were recorded at specified periods after 40 days of drying.

RESULTS AND DISCUSSION

Characterization of the Flax Fiber after Treatment

The schematics showing the chemical and structural modification in the flax fiber are given in Figure 2. In alkaline treatment, the noncellulosic cementing content (i.e., lignin and hemicellulose) of the flax was removed. As a result, cellulose underwent a new polymorphic structure, such that the crystals rearranged from cellulose I, in which the chains were aligned in parallel conformation, to cellulose II, in which the chains were antiparallel to each other^{28,29} [Figure 2(a)]. The chemical structure of the cellulose stayed the same, but the physical structure was modified. In the silanization of flax fibers, silanols reacted with the hydroxyls of cellulose; as a result, the fiber surface was organically functionalized [Figure 2(b)].

To monitor the structural changes in the flax fiber, Fourier transform infrared spectroscopy and XRD analysis were performed. The XRD patterns of the untreated, alkaline-treated, and silane-treated flax fibers are shown in Figure 3. The untreated fibers showed the main characteristic diffractions of cellulose I, [101] diffraction at $2\theta = 14^\circ$, [101'] diffraction at $2\theta = 15.5^\circ$, and [002] diffraction at $2\theta = 23^\circ$. The alkaline-treated flax fibers represented typical diffraction peaks, [101], [021], and [002] of cellulose II at $2\theta = 14$, 20, and 23° , respectively. The intensities of the [101'] and [002] diffraction peaks decreased, and the intensities of [021] diffractions increased in comparison to those of the untreated flax fiber. In addition, a peak appeared between and 60° ; this corresponded to the amorphous part of cellulose broadening. These findings pointed out

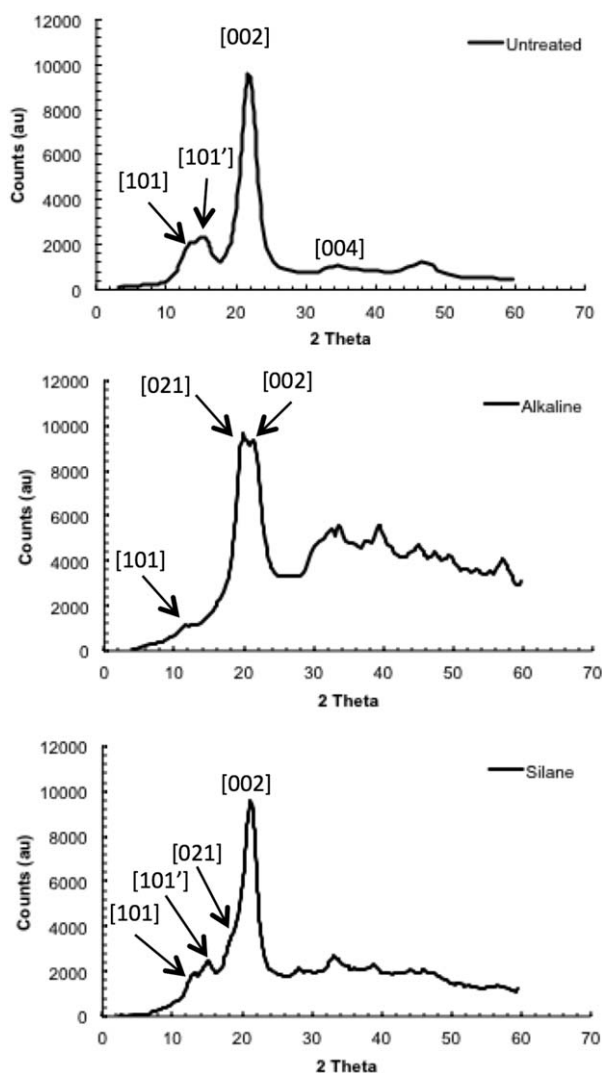


Figure 3. XRD patterns of the untreated, alkaline-treated, and silane-treated flax fibers.

that the crystalline ordered structure of the flax fibers were shifted to a disordered structure after alkaline treatment. These results are in good agreement with the literature.^{28,29} In the silane-treated fibers, the diffractogram mostly resembled the untreated flax fiber, except one for weak indication of the formation of the cellulose II structure, which was observed from the diffraction appearing at $2\theta = 20^\circ$ (the shoulder peak) for [021] of cellulose II. This gave the idea that the alignment of the cellulosic structure was slightly disturbed during silane treatment, probably because of the swelling of the flax fibers in the presence of the EtOH/water mixture.

An XPS analysis of the flax fibers was conducted to monitor whether silanization had taken place. XPS spectra results for the untreated and treated fibers are shown in Figure 4, and the elemental breakdown for the untreated, alkaline-treated, and silanized flax fiber is summarized in Table II. The main features observed in the spectra for the untreated and alkaline-treated flax fiber could be associated with the C1s and O1s photoelectrons; this indicated the saturated carbons and oxygen of cellulose.

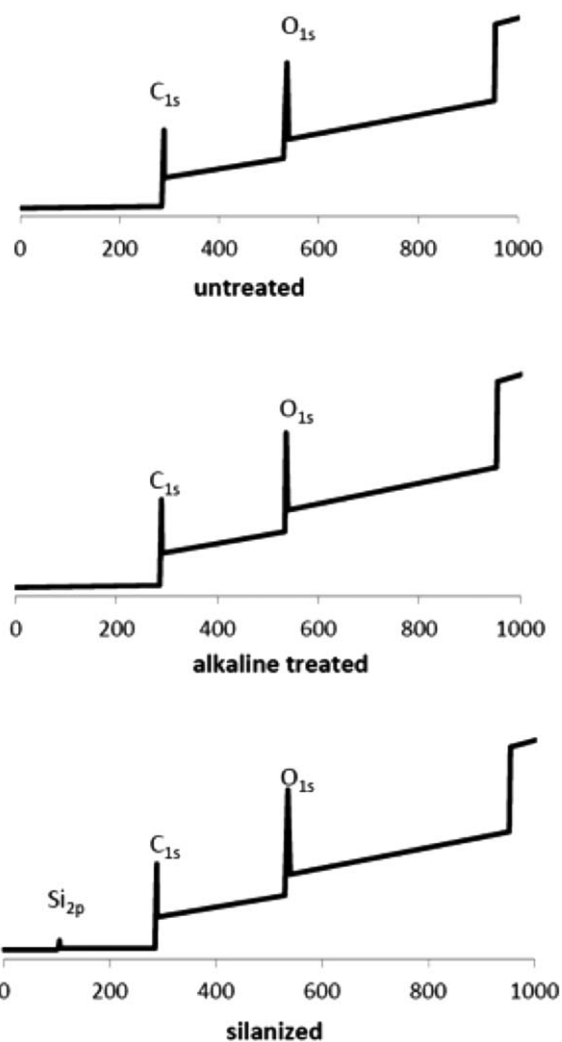


Figure 4. XPS scans for the untreated, alkaline-treated, and silanized flax fibers (the x axis shows the binding energy in electron volts).

lose. For the silanized fiber, in addition to the common C1s and O1s photoelectrons, there was clear evidence from the observation of the Si2p peak at 105 eV; this indicated the presence of silane group on the fiber surface. In addition, the amount of oxygen on the surface decreased because of the presence of silanes on the surface of the flax fiber (Table II).

The surface topologies of the untreated and alkaline- or silane-treated flax fibers are shown in Figure 5(a–c). We observed that the elementary fibers forming the untreated flax fiber were

Table II. Results of XPS Analysis

	Mass concentration (%)		
	O	C	Si
Untreated fiber	38.3	61.7	—
Alkaline treatment	39.7	60.3	—
Silane treatment	35.3	62.5	2.2

The binding energies were 536 eV for O, 289 eV for C, and 105 eV for Si.

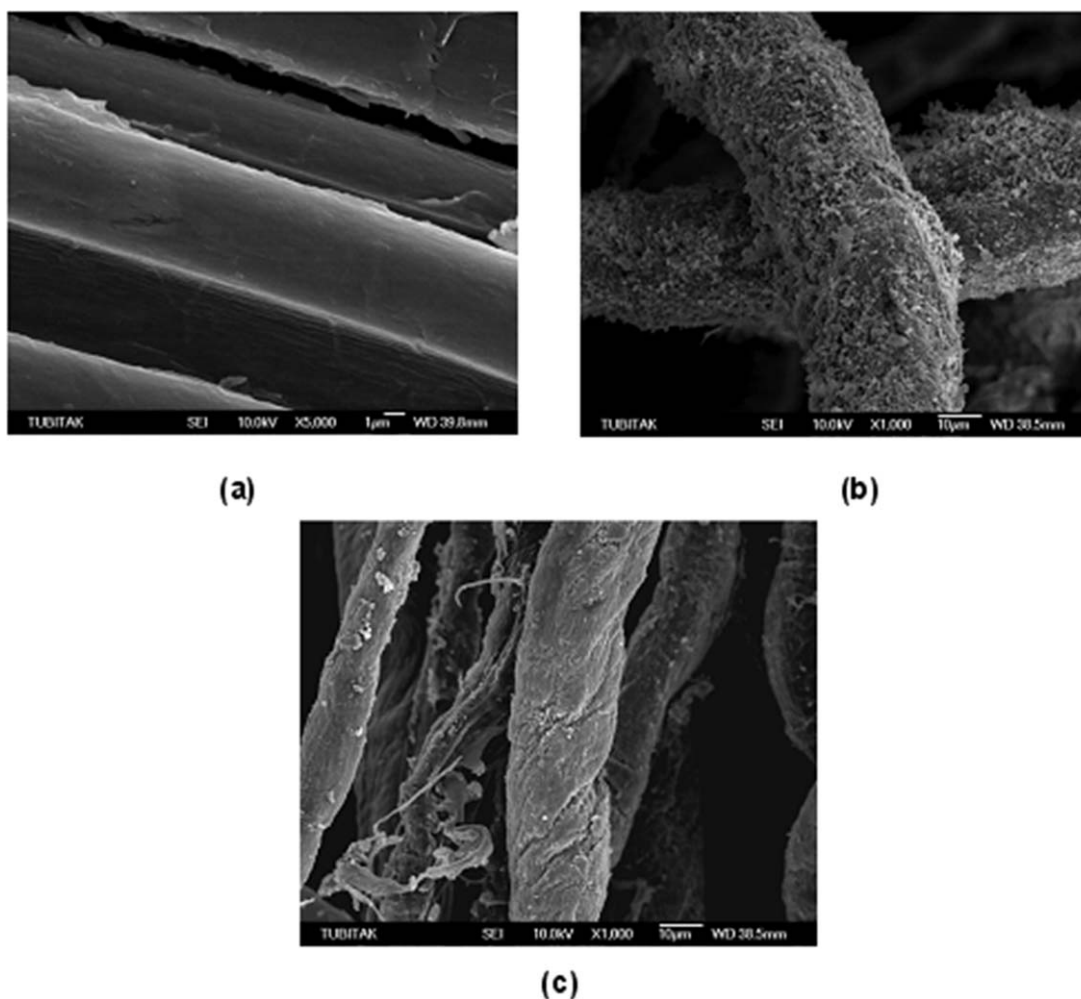


Figure 5. SEM micrographs of the (a) untreated (5000 \times), (b) alkaline-treated (1000 \times), and (c) silane-treated flax fibers (1000 \times).

aligned together. They seemed to be highly packed. After alkali treatment, this structure was deteriorated by the removal of noncellulosic materials [Figure 5(b)]. The elementary fibers were separated from each other. We observed that the surface roughness of the alkali-treated flax fibers were much higher in comparison to the untreated and silane-treated fibers. The fibrils were also separated from each other for silane-treated flax fiber, as shown in Figure 5(c). The surface of the silanized fibers was rougher in comparison to the untreated flax fibers. The rough, undulated structure seen on the fiber surface may have been due to the deposition of the silane layer on the surface.

Fiber Length Distribution

The importance of the critical fiber length in the mechanical performance of short-fiber composites has been shown in the literature. This critical aspect ratio (or length/diameter) depends on the intrinsic characteristics of the fiber, the matrix properties, and the strength of the fiber/matrix interphase.³⁰ The full performance of the composite was observed when the average length of the fibers was greater than a critical value after compounding. When the interfacial adhesion was high and the stress transfer was efficient, the required critical aspect ratio could be lower. However, in reality, the average fiber length

(AFL) of the composites was generally lower than the critical length. This means that the advantage of the fiber reinforcement capabilities could not be totally achieved.

The fiber breakage mechanism in the well-known system of chopped glass fiber/thermoplastic composites can be explained as follows: in shear flow, fibers are subjected to compressive forces; this leads to rupture because of buckling when the fibers are above a critical value.^{31,32} The fiber–fiber and fiber–metal collisions also induce fiber breakage. On contrary, the rupture mechanism is different for natural fibers³² because they are very flexible in comparison to glass fibers. They mostly tend to entangle under shear flow rather than breakage. Severe mixing conditions, such as higher rotor speeds, higher temperatures, and longer residence times, affect adversely AFL in natural-fiber-reinforced polymer composites.³³ The rupture of natural fibers seems to occur after an accumulation of fatigue by the time.³² An important structural property of flax fibers is the presence of repeating transversal defects due to the growth of cell walls and the extraction processes. These defects, called *kink bands*, play an important role in fiber rupture³⁴ (Figure 6). These defects act like sites for the initiation of fiber breakage and are responsible of the formation of microcracks.³⁵ A

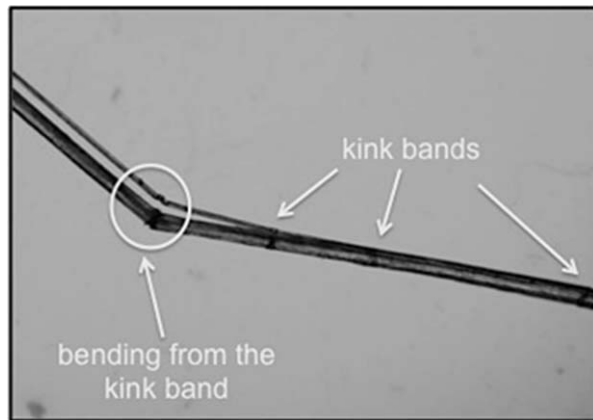


Figure 6. Optical micrograph of a flax fiber.

detailed work on the rupture mechanism of flax fibers has been published elsewhere.³²

Figure 7 shows the fiber length distribution of the untreated, alkaline-treated, and silanized flax fibers after processing. AFL for all three types of fiber decreased severely from 5 mm to approximately 0.3 mm because of the phenomena explained previously. AFLs for silanized and untreated fibers were around 300 μm (327 and 303 μm , respectively); but the smallest AFL was obtained for the alkaline-treated fibers as 265 μm . This was attributed to the surface defects formed after alkaline treatment, which weakened the fiber. It was reported that alkaline treatment may have decreased the mechanical properties of the fiber.³⁶ On the contrary, it was mentioned in the literature that silane treatment does not damage the natural fibers because no acidic or basic components are present nor is a high temperature used.³⁷

Figure 8 shows the fiber length distribution and AFL of alkaline-treated then polymer-coated flax fiber composites, and silane-treated then polymer-coated flax fiber composites. As shown in the histograms that the distribution curves shifted to the right (i.e., higher fiber length region) when PC was applied. As a result of this, the AFL values were higher in the case of PC in comparison to only alkaline treatment or only silane treatment. AFL increased approximately 200 μm (from 265 to 432 μm for alkaline treatment and from 327 to 493 μm) when PC was applied on silanized or alkaline-treated fibers. This increment was associated with the protective effect of the film former on the fiber surface. It is known from the literature that significant fiber breakup occurs right after the addition of fibers to the molten matrix.³⁸ The presence of a protective polymer layer or, in other words, a film former over the fiber surface may retard the break-up process.

Stress–Strain Behavior and Mechanical Properties of Composites

The stress–strain curves of the neat PLA and its flax fiber composites are given in Figure 9 with respect to the surface-treatment method. PLA exhibited yielding and subsequent short cold-flow region before failure. On the other hand, the stress–strain behavior of the flax fiber composites were different than that of neat PLA. In this case, failure occurred right after the

yielding process without any cold flowing because of the restricted chain slippage in the presence of flax fibers. The yield strength and elongation during yielding in the fiber-reinforced composites were strongly affected by the quality of the interphase. In the presence of a good adhesion, for a relatively ductile matrix, the yield strength was expected to be higher because the separation of the fiber–polymer interphase was delayed, and more load was transferred from the matrix to the fiber; this resulted in a higher yield strength and higher extent of deformation, that is, the yield strain, during tensile testing. By taking this phenomenon into account, the lower yield strength and elongation at yield obtained for the untreated and alkaline-treated flax fiber composites was attributed to the lack of

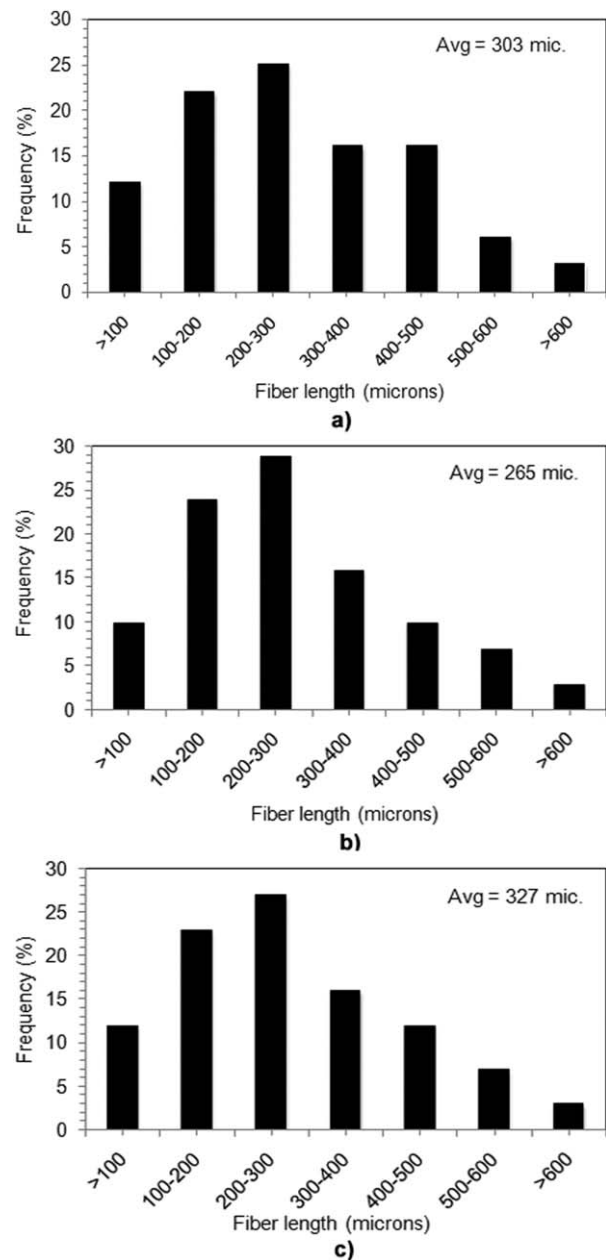


Figure 7. Fiber length distributions of the (a) untreated, (b) alkaline-treated, and (c) silane-treated uncoated flax fiber composites.

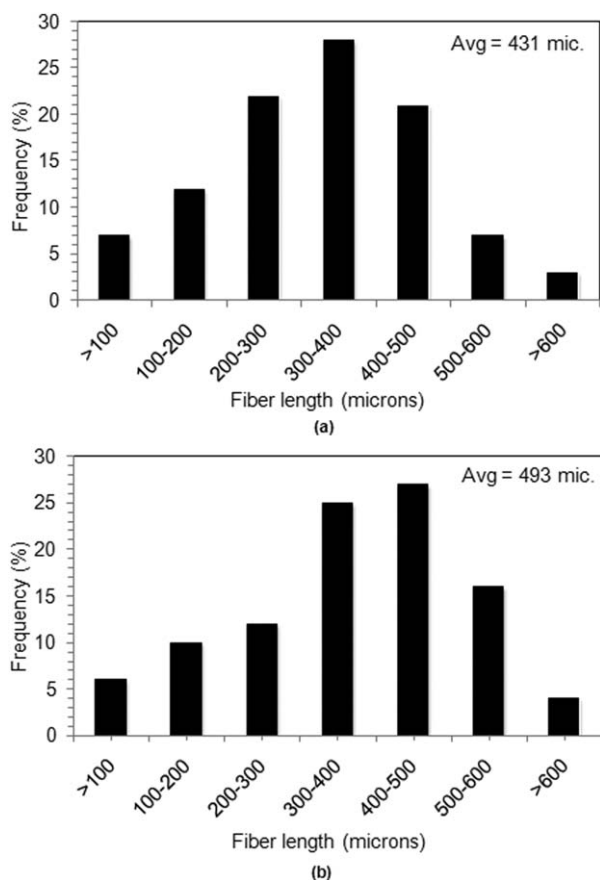


Figure 8. Fiber length distributions of the (a) alkaline-treated and polymer-coated flax fiber composites and (b) silane-treated and polymer-coated flax fiber composites.

interfacial interaction at the fiber–matrix interphase. The addition of the silane-treated flax fibers to PLA increased the yield strength and elongation at yield because of the possible physical or chemical interactions between the $-\text{NH}_2$ groups of APS and $-\text{COOH}$ end groups of PLA. In addition to the single influence of the silane coupling agent, the synergetic effect with PC was obvious in the stress–strain curves (see curve silane + PC). PC after both alkaline or silane treatment enhanced the yield strength and elongation at yield. This improved strength was associated with the enhanced interaction between the matrix and the silane coupling agent. When the silanized flax fiber was coated with PLA solution, the extended chains of PLA in solution could easily intermingle between the silane groups attached to the surface of the flax. This already interpenetrated structure could easily create chemical bonds during melt processing. On the other hand, only silanized flax fiber could not make proper contact because of the high viscosity of the molten matrix.

The overall picture of the tensile strength with respect to the surface-treatment technique is shown in Figure 10. In addition to the level of interfacial adhesion between the flax fiber and matrix, the resulting fiber length also displayed crucial importance to the mechanical properties of short-fiber-reinforced composites.³⁰ Because of the stress concentration at the ends of the fibers, matrix crack formation started at these points under tensile loading. As the strain was increased, more cracks were

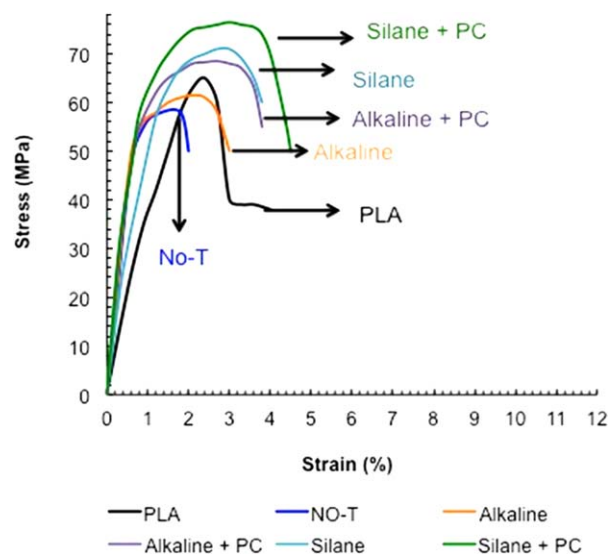


Figure 9. Representative stress–strain curves of the neat PLA and its flax fiber composites with respect to the surface-treatment type (No-T, no treatment). [Color figure can be viewed in the online issue, which is available at wileyonlinelibrary.com.]

formed. The cracking at the beginning of the tensile test may have been related to the load transfer to the fibers that connected the cracked regions. It is claimed in the literature that when the extent of cracking on the specimen reached a critical level and the surrounding fibers and matrix could no longer support the increasing load, the failure of the specimen occurred in the weakest region.^{39–41} As the fiber length decreased, the number of fiber ends increased; in other words, the number of stress concentrators increased in the matrix. Therefore, the composite failed earlier than in composites having shorter chains. This phenomenon was also effective in the current case, where the composites having a bigger AFL exhibited a higher tensile strength.

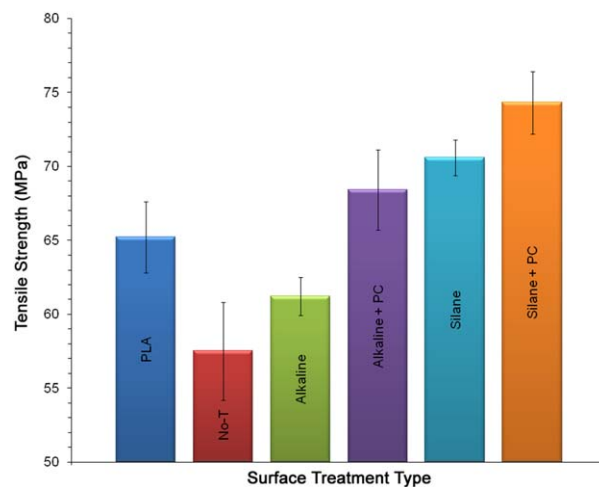


Figure 10. Tensile strength with respect to the surface-treatment type. [Color figure can be viewed in the online issue, which is available at wileyonlinelibrary.com.]

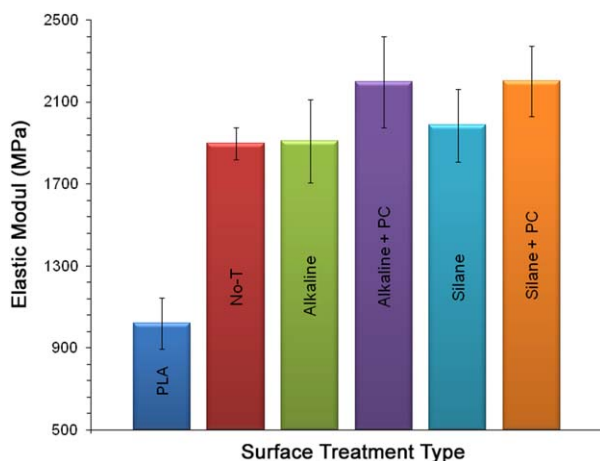


Figure 11. Elastic modulus with respect to the surface-treatment type. [Color figure can be viewed in the online issue, which is available at wileyonlinelibrary.com.]

The variation of the elastic modulus on the fiber surface treatment is shown in Figure 11. One should note that the elastic moduli of all of the composites were higher with respect to neat PLA. The elastic moduli of the short-fiber-reinforced composites depended on the fiber volume fraction and fiber efficiency factor, including the fiber orientation and fiber length.⁴² In other words, the interphase was not a major factor in the elastic modulus because the modulus was measured at very low strains. We observed that the elastic modulus data supported this phenomenon (Figure 11). The elastic modulus of the untreated, silane-treated, and alkaline-treated flax fiber composites and alkaline-treated/polymer-coated and silane-treated/polymer-coated flax fiber composites were similar. In addition, the polymer-coated fibers exhibited improved the elastic modulus because the AFL was higher than that of the uncoated fibers.

Dynamic Mechanical Properties and Impact Testing

To observe the heat-dependent dynamic mechanical properties of the flax fiber composites, dynamic mechanical analysis was conducted in temperature sweep mode. The change in the storage modulus and loss factor with respect to the temperature of the selected composites are shown in Figure 12(a,b), respectively. The positive influence of the surface treatment on the storage modulus of the composites was easily observed [Figure 12(a)]. It was obvious that incorporation of flax fibers to neat PLA resulted in an increase in the stiffness of the composites at room temperature and also at elevated temperatures. In other words, this observation indicated that the flax fiber composites had improved thermomechanical resistance compared to that of PLA. As the type of surface treatment was focused, the silanized and polymer-coated flax fiber composites exhibited higher stiffness in the glassy and rubbery regions.

The glass-transition temperature (T_g) of PLA in the composites was higher than that of the neat PLA. This was due to the restriction of the chain movements in the presence of the flax fibers. The damping peak of PLA in the composites shifted to higher temperatures with surface treatment. The lowest T_g was obtained in the untreated flax fiber composites among the three

selected composites. T_g was found to be 74°C when flax fibers were silanized and polymer-coated. This value was 7°C higher than that of neat PLA. The damping peak in the composites of treated fibers showed a decreased magnitude of loss factor in comparison to the untreated composites. That was why the fibers could carry a greater extent of stress and allowed only a small part of it to strain the interphase; therefore, energy dissipation occurred in the matrix and at the interphase. This indicated that a stronger interface could be characterized by less energy dissipation, that is, a lower magnitude of the loss factor. In other words, the composite with poor interfacial bonding between the fibers and matrix tended to dissipate more energy; it showed a high magnitude of the damping peak in comparison to a material with a strongly bonded interface. This phenomenon was clearly observed in this case. The damping peak for the silanized and polymer-coated flax fiber composites

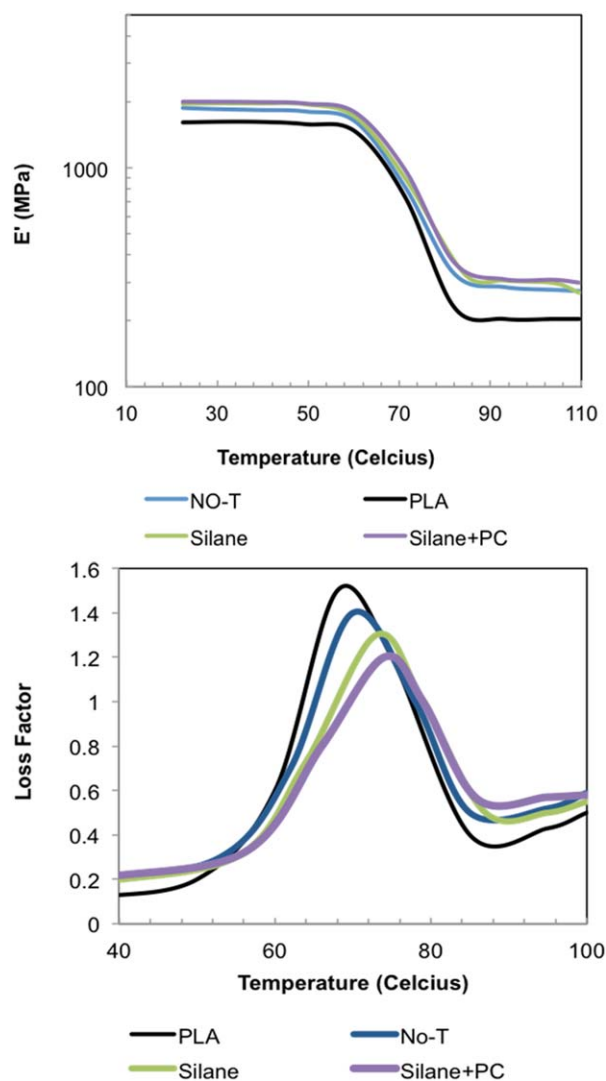


Figure 12. Dynamic mechanical analysis of the neat PLA, untreated flax composites, silanized flax composites, and silanized/polymer-coated flax composites: (a) storage modulus (E') and (b) loss factor. [Color figure can be viewed in the online issue, which is available at wileyonlinelibrary.com.]

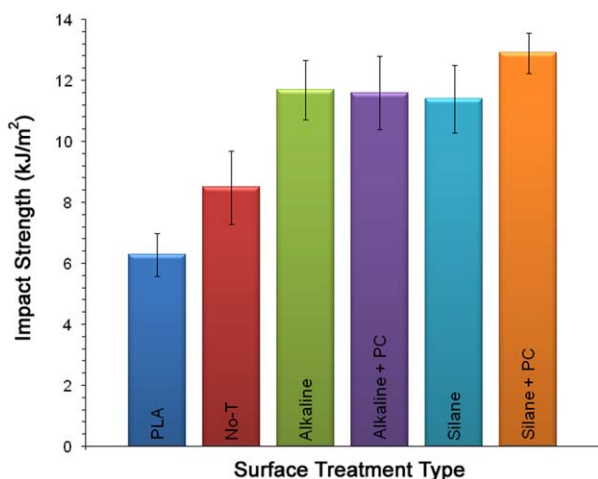


Figure 13. Impact strength with respect to the surface-treatment type. [Color figure can be viewed in the online issue, which is available at wileyonlinelibrary.com.]

exhibited the lowest magnitude of loss factor; this supported the fact that the interfacial interactions were the best among the others [see Figure 12(b)].

The change in the Charpy unnotched impact strength of the neat PLA and flax fiber composites is shown in Figure 13. We observed that the impact strength of all of the composites were higher than those of the neat PLA, regardless of the treatment

type. This finding was parallel to findings the literature.⁴³ The highest impact strength was obtained in the silanized and polymer-coated flax fiber composites. The increase in this composite was approximately twofold in comparison to neat PLA. This was attributed to the better interfacial interaction, which needed more energy during crack propagation under impact testing and higher AFL.

Interfacial Morphology by SEM

SEM micrographs showed the tensile fractured surfaces of the SFF composites (Figure 14). In the case of the untreated flax fibers, the fiber surfaces were smooth and clean; this showed a lack of interaction between the fiber and PLA matrix [Figure 14(a)]. The black line (marked with a circle) seen around the fiber on the matrix was due to the deconstruction of the fiber–matrix interface, the so-called *debonding* of the fiber under a tensile load.⁴⁴ For such a system, failure was accompanied by the pullout of fibers from the matrix. On the other hand, it was clear from the SEM micrographs that the surface of the flax fibers either silanized or silanized/polymer-coated were covered by a polymer layer; this was evidence of a strong interaction. In the case of a strong interphase, the density of the matrix near the fiber surface was different than those of the bulk polymer; therefore, the failure under tensile loading occurred at the matrix near the fibers. The polymer-coated fibers shown in the SEM micrographs (marked with a circle) were probably due to this failure mechanism.

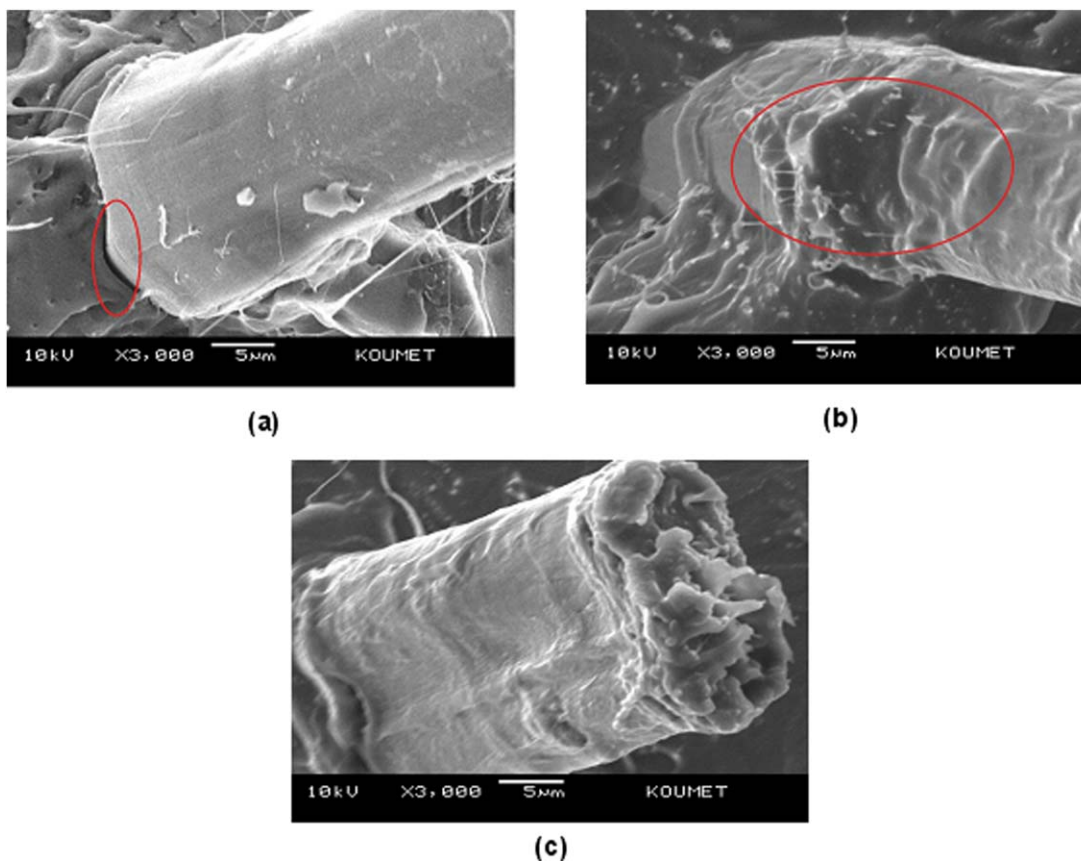


Figure 14. SEM micrographs of the flax fiber composites: (a) untreated, (b) silane-treated, and (c) silane-treated and polymer-coated. [Color figure can be viewed in the online issue, which is available at wileyonlinelibrary.com.]

Table III. Results of the DSC Analysis

Treatment type	T_g (°C)	T_{cc} (°C)	T_m (°C)	Crystallinity (%)
PLA	67.8	—	—	—
Untreated	66.3	132.3	151.6	3.5
Alkaline	65.9	131.8	152.9	2.7
Alkaline + PC	68.1	124.7	154.6	5.6
Silane	66.2	132.3	153.1	3.1
Silane + PC	65.6	127.7	154.8	5.3

Thermal Properties by DSC Analysis

The results of DSC analysis are listed in Table III. As shown, both T_g and T_m of the neat PLA and the composites did not exhibit any significant change with respect to the fiber surface-treatment technique. One also should note that the entire composites had a very low amount of crystallinity; this ranged between 2.7 and 5.3%. The main difference was obtained in the cold crystallization behavior of the composites. We observed that the cold crystallization temperature (T_{cc}) values of the untreated and alkaline- or silane-treated flax fiber composites were the same, but the alkaline-treated/polymer-coated and silane-treated/polymer-coated flax fiber composites had a significantly lower T_{cc} value. This indicated the nucleating effect of these flax fibers; this was possibly due to the much easier nuclei formation because of the already immobilized PLA chains on the surface of the PLA coated and chemically modified flax fibers. This could be an advantage in the injection-molding process for shortening the cycle times.

Hydrolytic Degradation

Figure 15 shows the percentage of weight loss as a function of the hydrolytic degradation time for the PLA and flax fiber composites. We observed that the weight loss curves could be divided into three categories: (1) neat PLA; (2) untreated or alkaline- or silane-treated flax fiber composites; and (3) silanized or alkaline-treated and polymer-coated flax fiber composites. Because of its relatively lower hydrophilicity, the hydrolysis rate of PLA was the lowest with respect to the flax fiber composites. The weight loss of PLA in the first 10 days was around 2%; then, the hydrolysis rate increased in the last 20 days. In total, the PLA lost approximately 35% of its initial weight at the end of the test of 40 days.

Natural fibers are highly hydrophilic in nature, and they easily absorb water. Therefore, the incorporation of natural fibers into polymeric matrices will generally increase the hydrophilicity of the resulting composite.⁴⁵ The untreated, alkaline-treated, and silanized flax fiber composites exhibited a similar trend in the hydrolytic degradation time. In the first 10 days of the experiment, they lost approximately 20% of their initial weight. This sharp weight reduction continued until 60% of weight loss was reached. In comparison to the neat PLA, the composites exhibited a higher amount of weight loss during the test. The presence of flax fibers accelerated the hydrolysis rate of the composites; this agreed with the results reported in the litera-

ture.^{46–49} This was because water could easily penetrate from the edges of the composites in the flax-based samples because flax behaved as a channel for the water to penetrate inside the composite. In addition, such a finding was sensible, given the hydrophobic nature of PLA and the hydrophilic nature of the flax fiber. Despite the high rate of weight loss, the silane-treated flax fiber composites showed a relatively slower degradation rate in comparison to the untreated and alkaline-treated flax fiber composites. This observation was attributed to the relatively lower hydrophilicity of the silane-treated flax fibers and better polymer–fiber interphase.

Silane- or alkaline-treated and polymer-coated flax fiber composites showed a lower weight loss with respect to the untreated and alkaline- and silane-treated flax fiber composites. This behavior was associated with the reduced hydrophilicity of the fibers and the improved interphase due to polymer pre-coating. The values of weight loss for any given period of time was the same for the silanized and alkaline-treated then for the polymer-coated flax fibers. They both exhibited a 50% weight loss at the end of 40 days.

Quantitative Comparison of the Current Composites with the Literature

There are several promising markets for biodegradable polymers such as PLA. Plastic bags and barriers for sanitary products, such as diapers, disposable cups, and plates, are some commodity applications. In addition, plastics used in white goods or automotive applications could be a high-value-added potential market for biodegradable composites. Because PLA can be processed in nearly the same way as PP, it is possible to replace PP composites with PLA/SFF composites that can be prepared via twin-screw extrusion.

The tensile properties and impact strength of the polymer-coated and silanized flax fiber/PLA biodegradable composites, which exhibited the highest properties in this study, were compared with nonbiodegradable (mostly PP based) and

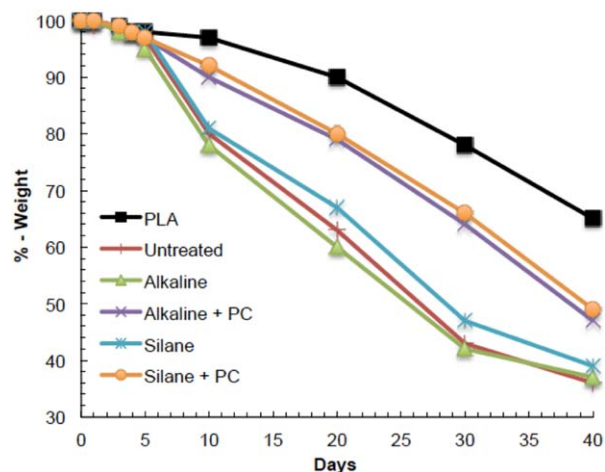


Figure 15. Weight loss in hydrolytic degradation with time (days). [Color figure can be viewed in the online issue, which is available at wileyonlinelibrary.com.]

Table IV. Comparison of Current Composites with Selected Biodegradable and Nonbiodegradable Composites

Composite description and source	Fiber content	Tensile strength (MPa)	Impact strength (kJ/m ²)	Elongation at break (%)
Silane-treated and polymer-coated SFF PLA composites (this study)	25 wt %	74.3	12.7	2.2
PLA/SFF ⁹	40 wt %	44	12	0.9
PLA/Biotex flax fiber composites (continuous woven flax fiber textile reinforcement, 250 tex) ⁵⁰	40 vol %	102	32.8	1.6
PLA/polycarbonate (10%)/NaOH-treated SFF ⁵¹	10 wt %	53 ^a	—	—
PLA/randomly scattered nonwoven SFF ⁵²	20 vol %	72 ^a	—	1.7 ^a
PP/maleated PP (5%)/SFF (extrusion compounding) ⁵³	30 wt %	39 ^a	—	—
PP/SFF ⁹	40 wt %	29	—	1.5

^aObtained from the graph.

biodegradable flax fiber-reinforced composites (see Table IV). One should note that some of the composites contained SFF, but some contained woven or nonwoven flax fibers.

Despite the lower content (25 wt %) of flax fiber in these composites, the tensile strength was observed to be higher than the composites with the higher SFF content (40 wt %) without a loss in the toughness-related properties, such as the impact strength and tensile elongation at break. The usage of woven or nonwoven flax fibers was much stronger than these composites. This was a consequence of the presence of continuous or longer fibers. The challenging question here was what the properties of polymer-coated and silane modified continuous flax fiber composites would be. On the other hand, as the properties of current composites were compared with that of the flax fiber/PP nonbiodegradable composites, we observed that the properties were much higher than those of the PP composites.

The benefit to the use of a film former over the flax fiber surface after chemical treatments was the ease of handling and feeding. Figure 16 shows the pictures of the silanized flax fibers after chopping. The one coated by a film former (PLA layer) kept its granular form; this helped in feeding to the compounder like glass fibers, but the one without film former turned to a mass of fluffy fibers of which it was very difficult to feed with conventional feeding systems.



Figure 16. Pictures of the chopped flax fibers: (a) silanized and polymer-coated and (b) silanized. [Color figure can be viewed in the online issue, which is available at wileyonlinelibrary.com.]

CONCLUSIONS

The combinatorial effect of the chemical surface modification via alkaline treatment or silanization and PC as the application of the film former on the physical and mechanical properties of the SFF/PLA composites were investigated. Both the alkaline and silane treatment affected the structure of the flax fiber. XRD analysis shows that the alkaline treatment changed the cellulose I structure into a cellulose II structure. It was revealed from the XPS analysis that the silane treatment was successfully implemented to the fiber. The mechanical tests showed that the usage of PC on the modified flax fiber surface enhanced the performance of the composite. The maximum tensile and impact strengths were obtained in the silanized and polymer-coated flax fiber composites. Moreover, it was shown that the thermomechanical resistance of this composite system was the highest among the others. DSC analysis indicated that the cold crystallization process of PLA was affected by the different surface treatments of the flax fibers. The presence of PC enhanced the crystallization of PLA in the composites without deteriorating the T_m and T_g values of the system. PC negatively affected the hydrolysis behavior of the flax fiber composites by decreasing the hydrophilicity of the flax fibers. We concluded that in particular, in addition to the single influence of the silane coupling agent, a synergetic effect of the film former (i.e., PC) and silane treatment was observed to improve the performance of the composites.

REFERENCES

- Hu, R.-H.; Sun, M.-Y.; Lim, J.-K. *Mater. Des.* **2010**, *31*, 3167.
- John, M. J.; Anandjiwala, R. D. *Compos. A* **2009**, *40*, 442.
- Aydın, M.; Tozlu, H.; Kemaloglu, S.; Aytac, A.; Ozkoc, G. J. *Polym. Environ.* **2011**, *19*, 11.
- Li, X.; Tabil, L. G.; Panigrahi, S. J. *Polym. Environ.* **2007**, *15*, 25.
- Lau, K. Presented at the 16th International Conference on Composite Materials, July 2007, Kyoto.

6. Wang, K. H.; Wu, T. M.; Shih, Y. F.; Huang, C. M. *Polym. Eng. Sci.* **2008**, *48*, 1833.
7. Iannace, S.; Nocilla, G.; Nicolais, L. *J. Appl. Polym. Sci.* **1999**, *73*, 583.
8. Plackett, D.; Andersen, T. L.; Pedersen, W. B.; Nielsen, L. *Compos. Sci. Technol.* **2003**, *63*, 1287.
9. Oksman, K.; Skrifvars, M.; Selin, J. F. *Compos. Sci. Technol.* **2003**, *63*, 1317.
10. Bax, B.; Müssig, J. *Compos. Sci. Technol.* **2008**, *68*, 1601.
11. Baley, C.; Busnel, F.; Grohens, Y.; Sire, O. *Compos. A* **2006**, *37*, 1626.
12. Raj, G.; Balnois, E.; Baley, C.; Grohens, Y. Presented at the International Conference on Composite Materials, July **2009**, Edinburgh, Scotland.
13. Zhu, J.; Zhu, H.; Njuguna, J.; Abhyankar, H. *Materials* **2013**, *6*, 5171.
14. Di Bella, G.; Fiore, V.; Valenza, A. *Mater. Des.* **2010**, *31*, 4098.
15. Chabba, S.; Netravali, A. N. *J. Mater. Sci.* **2005**, *40*, 6263.
16. Van de Weyenberg, I.; Ivens, J.; De Coster, A.; Kino, B.; Baetens, E.; Verpoest, I. *Compos. Sci. Technol.* **2003**, *63*, 1241.
17. Sirvaitiene, A.; Jankauskaite, V.; Bekampiene, P.; Kondratas, A. *Fiber. Text. East. Eur.* **2013**, *21*, 123.
18. Ku, H.; Wang, H.; Pattarachaiyakoop, N.; Trada, M. *Compos. B* **2011**, *42*, 856.
19. Mishra, S.; Misra, M.; Tripathy, S. S.; Nayak, S. K.; Mohanty, A. K. *Polym. Compos.* **2002**, *23*, 164.
20. Yuan, Y.; Guo, M.; Wang, Y. *Intell. Comput. Inf. Sci.* **2011**, *134*, 547.
21. Le Moigne, N.; Longerey, M.; Taulemesse, J.-M.; Benezet, J.-C.; Bergeret, A. *Ind. Crop Prod.* **2014**, *52*, 481.
22. Thomason, J. L. Presented at the 28th Riso International Symposium on Material Science: Interface Design of Polymer Matrix Composites—Mechanics, Chemistry, Modelling and Manufacturing, **2007**, Roskilde, Denmark.
23. Mader, E. *Compos. Sci. Technol.* **1997**, *57*, 1077.
24. Mai, K.; Mader, E.; Muhle, M. *Compos. A* **1998**, *29*, 1111.
25. Thomason, J. L.; Adzima, L. *J. Compos. A* **2001**, *32*, 313.
26. Wu, H. F.; Dwight, D. W.; Huff, N. T. *Compos. Sci. Technol.* **1997**, *57*, 975.
27. Altun, Y.; Doğan, M.; Bayramlı, E. *J. Polym. Environ.* **2013**, *21*, 850.
28. Qin, C.; Soykeabkaew, N.; Xiuyuan, N.; Peijs, T. *Carbohydr. Polym.* **2008**, *71*, 458.
29. Ouajai, S.; Hodzic, A.; Shanks, R. A. *J. Appl. Polym. Sci.* **2004**, *94*, 2456.
30. Kelly, A.; Tyson, W. R. *J. Mech. Phys.* **1965**, *13*, 329.
31. von Turkovich, R.; Erwin, L. *Polym. Eng. Sci.* **1983**, *23*, 743.
32. Le Duc, A.; Vergnes, B.; Budtova, T. *Compos. A* **2011**, *42*, 1727.
33. Joseph, P. V.; Joseph, K.; Thomas, S. *Compos. Sci. Technol.* **1999**, *59*, 1625.
34. Wang, H. M.; Wang, X. *Fibers Polym.* **2005**, *6*, 6.
35. Baley, C. *J. Mater. Sci.* **2004**, *39*, 331.
36. Arbelaiz, A.; Cantero, G.; Fernandez, B.; Mondragon, I. *Polym. Compos.* **2005**, *26*, 324.
37. Sreekala, M. S.; Kumaran, M. G.; Thomas, S. *J. Appl. Polym. Sci.* **1997**, *66*, 821.
38. Ville, J.; Inceoglu, F.; Ghamri, N.; Pradel, J. L.; Durin, A.; Valette, R.; Vergnes, B. *Int. Polym. Proc.* **2013**, *28*, 49.
39. Fu, S. Y.; Lauke, B.; Mader, E.; Yue, C. Y.; Hu, X. *Compos. A* **2000**, *31*, 1117.
40. Sato, N.; Kurauchi, T.; Sato, S.; Kamigaito, O. *J. Mater. Sci.* **1984**, *19*, 1145.
41. Takahashi, K.; Choi, N. S. *J. Mater. Sci.* **1991**, *26*, 4648.
42. Ozkoc, G.; Bayram, G.; Bayramli, E. *Polym. Compos.* **2005**, *6*, 745.
43. Rawi, N. F. M.; Jayaraman, K.; Bhattacharyya, D. *Polym. Compos.* **2004**, *35*, 1888.
44. Landel, R. F.; Nielsen, L. E. *Mechanical Properties of Polymers and Composites*, 2nd ed.; Marcel Dekker: New York, **1994**.
45. Bismarck, A.; Aranberri-Askargorta, I.; Springer, J. *Polym. Compos.* **2002**, *23*, 872.
46. Cao, Y.; Shibata, S.; Goda, K. *Key Eng. Mater.* **2007**, *221*, 334.
47. Wu, C. S. *J. Appl. Polym. Sci.* **2006**, *102*, 3565.
48. Wang, R.; Wang, C. H.; Jiang, Z. H. *J. Fiber Bioeng. Inf.* **2010**, *3*, 75.
49. Bayerl, T.; Geith, M.; Somashekar, A.; Bhattacharyya, D. *Int. Biodeterior. Biodegrad.* **2014**, *96*, 18.
50. Siengchin, S.; Pohl, T.; Medina, L.; Mitschang, P. *J. Reinf. Plast. Compos.* **2013**, *32*, 23.
51. Karsli, N. G.; Aytac, A. *Fiber Polym.* **2014**, *15*, 2607.
52. Bodros, E.; Pillin, I.; Montrelay, N.; Baley, C. *Compos. Sci. Technol.* **2007**, *67*, 462.
53. Arbelaiz, A.; Fernandez, B.; Cantero, G.; Llano-Ponte, R.; Valea, A.; Mondragon, I. *Compos. A* **2005**, *36*, 1637.